energies

MDPI

Review

A Review of On-Line Measurement Methods of Alkali Metal Emissions from Combustion by Passive Spontaneous Emission Spectroscopy

Weihui Liao [1], Chao Yan [1], Xingcheng Lyu [1], Yang Pu [2], Chun Lou [2,*] and Mooktzeng Lim [3]

[1] Guangdong Red Bay Generation Co., Ltd., Shanwei 516623, China
[2] State Key Laboratory of Coal Combustion, School of Energy and Power Engineering, Huazhong University of Science and Technology, Wuhan 430074, China
[3] Department of Mechanical Engineering, Faculty of Engineering and Quantity Surveying, INTI International University & Colleges, Nilai 71800, Negeri Sembilan, Malaysia
* Correspondence: lou_chun@sina.com or clou@hust.edu.cn; Tel.: +86-136-1863-9018

Abstract: This article reviews the principles and applications of passive spontaneous emission spectroscopy (SES) for the quantitative determination of alkali metal concentrations emitted from combustion processes. The combustion of fuels that contain a high alkali metal content (Na and/or K) is challenging, as alkali metals reduce the slag formation temperature and induce fouling, causing combustion facilities to shutdown prematurely. The in situ on-line quantification of alkali metals is, thus, a critical measure to control combustion processes, preventing slagging and fouling from occurring. This review shows that several SES systems, developed by the Huazhong University of Science and Technology (HUST), are inexpensive, portable, and useful for measuring the alkali metal content, and have been applied for biomass combustion as well as coal and municipal solid waste combustion, from laboratory-scale settings (20 kW) to industrial facilities (300 MW). Compared with other research, the SES system from HUST has successfully quantified the emitted alkali metal concentrations during combustion. This review also highlights the challenges of the SES system and recommends further work to improve it for further applications.

Keywords: high-alkali fuels; gaseous alkali metal concentration; temperature; on-line measurement; spontaneous emission spectroscopy

Citation: Liao, W.; Yan, C.; Lyu, X.; Pu, Y.; Lou, C.; Lim, M. A Review of On-Line Measurement Methods of Alkali Metal Emissions from Combustion by Passive Spontaneous Emission Spectroscopy. *Energies* **2022**, *15*, 9392. https://doi.org/10.3390/en15249392

Academic Editor: Alessandro Cannavale

Received: 1 November 2022
Accepted: 8 December 2022
Published: 12 December 2022

1. Introduction

Solid fuels such as coal, biomass, and municipal solid waste contain high concentrations of alkali metals such as sodium (Na) and/or potassium (K). From the combustion of these fuels, alkali metals are devolatilized in gaseous form. The gaseous alkali metals then condense on the metal surfaces of the heat exchangers in furnaces or boilers, causing fouling and slagging, reducing the heat transfer efficiency [1–3]. Once the slag layer reaches a certain thickness, the boiler or furnace needs to be shut down for maintenance, resulting in revenue losses. Analysis of the alkali metals in the ash in an offsite laboratory is time-consuming, depending on the distance from the plant (e.g., palm oil mills in Malaysia are located in remote areas). Even if the plant has an on-site instrument for performing standardized measurement methods, such as (but not limited to) an inductively coupled plasma mass spectroscope (ICP-MS) [4], the gaseous alkali metals would have nucleated and condensed in the ash deposits, or melted to form slags consisting of aluminosilicates [5,6]. Thus, in situ on-line quantitative measurements are needed to determine the gaseous concentration of the alkali metals in real time, allowing for instant operational mitigation measures to be implemented to avoid unplanned shutdown of the plant due to slagging and fouling.

Such on-line quantitative measurement systems have been investigated before. For example, Fatehi et al. [7] summarized recent numerical and experimental investigations of

biomass thermochemical conversion processes, where the alkali metal concentrations and temperature were measured using active and passive methods. Active methods include the measurement methods using an external excitation source, e.g., laser-based techniques such as planar laser-induced fluorescence (PLIF), laser-induced breakdown spectroscopy (LIBS), and absorption spectroscopy (AS) [7]. An external excitation source is needed to observe the spectral states of atoms and molecules in the combustion process. Due to their higher temporal and spatial resolution, active measurement methods have been widely used in laboratory combustion diagnosis [8–11]. However, active measurement methods are limited by their cost and relative difficulty in setting up, due to the need for precise alignment of the optical setup and excitation source. For instance, LIBS uses an excitation source to measure the gas-phase species of different species but only in a small, controlled volume [7]. Another study used a broadband excimer laser at an ultraviolet wavelength of 193 nm to produce excited alkali potassium and sodium. This system does provide data in real time, but the setup includes an automated filter wheel and an alignment device between the laser beam with glass fiber bundles [12].

Meanwhile, passive methods are based on the analysis of spontaneous emission spectroscopy (SES) from the flames [4], and are relatively cheaper and easier to set up, since the excitation source is the flame itself. For example, the spontaneous emissions from a $CH_4/H_2/CO$ flame (250 to 700 nm) were analyzed with a high-resolution optical spectrometer only. The spectrometer was placed such that the spectrum of the whole flame volume was analyzed, ignoring the effect of spatial variations [13]. Another study presented a portable in situ SES method to quantify the alkali metal emissions in terms of the ground-state relative number densities and the speciation between potassium and sodium from biomass combustion in a 100 kW furnace [14]. Similar methods have been deployed in industrial environments to determine the gaseous alkali metal concentrations in different combustion facilities [15,16].

Although passive measurement methods have been deployed, the following information is not readily available in the literature: (1) limited spatial and temporal profiles of gaseous alkali metal concentrations for large-scale industrial boilers due to line-of-sight-only constraints; (2) lack of quantitative measurements in industrial settings; and (3) lack of correlation between alkali metal concentration and combustion parameters. Therefore, the present paper reviews several deployments of the SES passive measurement method. First, this article describes the principles for the SES measurement method. Then, the investigation of gaseous alkali metals' devolatilization or emission characteristics in lab-scale facilities using SES is presented. A further section is dedicated to applications of SES in industrial settings. Temporal and spatial profiles of the gaseous alkali metal emissions, temperature, and other information are presented. Based on these examples, the challenges of the SES system are identified, and recommendations to address these challenges are discussed.

2. Principles and Setup

The spontaneous optical emission spectra from combustion are due to the electromagnetic radiation of particulates, gases, excited species, and free atoms in the flames. The radiation from the different components in the flames are summarized into line, band, and continuous spectra, respectively, ranging from the ultraviolet to the visible and infrared wavelengths. Depending on the type of fuel and parameters, every flame has its own characteristic spontaneous emission spectrum. For instance, solid particles such as soot or char emit a continuous spectrum in the visible and infrared wavelengths. This is also known as the blackbody radiative spectrum, and its intensity corresponds with the combustion temperature [17]. Thermal radiation from gases (mainly CO_2 and H_2O) emits in infrared wavelengths and demonstrates band emission characteristics. Excited free radicals such as OH* (309 nm), CH* (431 nm), C_2* (516 nm), and CO_2* (350–600 nm) emit radiation or chemiluminescence at the corresponding wavelengths due to de-excitation reactions. Fuels containing alkali metals emit atomic line spectra at the characteristic wavelengths [17].

From this radiation, better insights into the combustion pathways and reactions can be obtained. In addition, quantitative analysis of the flame's spontaneous emission spectrum (such as the line intensity and width) is used to determine the species concentrations and temperature [18–20]. This procedure is also used for the in situ real-time quantification of gaseous alkali metal concentrations. Figure 1 shows the setup for obtaining the spontaneous emission spectrum, consisting of a visual or optical access, a radiative collection lens or a collimating lens, a spectral splitter, and a photo-detector.

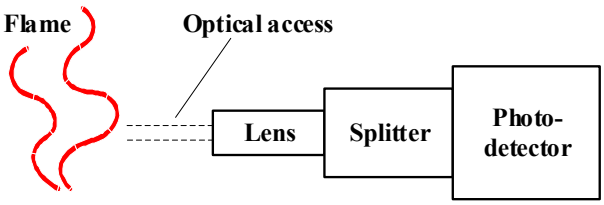

Figure 1. Schematic of emission measurement system.

There are two methods to perform SES. A typical configuration to investigate flame emission is by using a photo-multiplier tube or photo-diode associated with the band-pass filter. The optical band-pass filter isolates the characteristic wavelength of alkali metals in the flame, the intensity of which is recorded by the photo-multiplier tube or the photo-diode. A grating monochromator or spectrometer can also be used to replace the band-pass filter and the photo-multiplier tube/photo-diode for photo-detection [21,22]. Because each alkali metal (or a specific element) emits light at a characteristic wavelength [23], the wavelength range of the emission measurement system should cover these wavelengths, and the wavelength resolution should be sufficiently high to distinguish the different emission lines. The time resolution of the system is limited by the response time of the detector, the data acquisition, and processing capability. While the system only permits line-of-sight measurement and provides qualitative spectral information with low spatial resolution, quantitative or spatial information could be derived from the spontaneous emission spectra. However, as is discussed in further sections, if visual or optical access to the flame is available, the spatial profile of the target element or species is obtainable, even in an industrial-scale setting.

The spectrometer measures the spontaneous emission spectra in terms of photon counts with respect to the wavelength. The photo counts reflect the relative spectral intensity distribution and are calibrated to the absolute intensities. This can be achieved via a blackbody furnace, from which coefficients for the calibration curves are obtained. This is achieved by taking the ratio of spectral intensities from the blackbody furnace to the photo counts from the spectrometer. It should be noted that, beyond the alkali metal emission, there is a continuous blackbody radiation from the solid particles. Figure 2 shows the spectral radiative intensities I of high-alkali fuels' combustion collected by a spectrometer, composed of a continuous spectrum I_c and a discontinuous spectrum I_d.

Consequently, I can be expressed as the sum of I_c and I_d as follows [24]:

$$I(\lambda) = I_c(\lambda) + I_d(\lambda_{\mathrm{Li}}) + I_d(\lambda_{\mathrm{Na}}) + I_d(\lambda_{\mathrm{K}}) + I_d(\lambda_{\mathrm{Rb}}) \quad (1)$$

where I_c is the thermal radiation intensity, and I_d represents the spectral intensities of gaseous alkali metals such as Li, Na, K, and Rb. The continuous and discontinuous spectra are separated based on principal component analysis [25].

The continuous spectral radiation in the visible and near-infrared wavelengths approximates Planck's law of radiation, from which the combustion temperature can be determined [25–28]. The spectral intensities of the gaseous alkali metals can be calculated based on the spontaneous emission spectra. The devolatilized potassium and sodium in the flames are in an excited energy state. Therefore, the spectral intensities correspond to their gaseous concentrations [29]. In the next section, the application of SES for characterizing alkali metal emissions is presented.

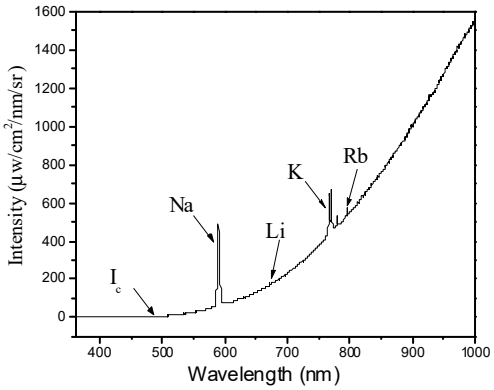

Figure 2. An example of a spectral radiative intensity from combustion of high-alkali fuels.

3. Application of SES for Quantitative Measurement of Gaseous Alkali Metals

3.1. Biomass Combustion

As an alternative energy to fossil fuels, biomass can be directly combusted to generate heat and power. However, certain types of biomass contain high concentrations of alkali metals such as potassium, which is an element in agricultural fertilizers useed to promote growth. Alkali metals reduce the temperature for the formation of slag. Thus, high potassium concentrations exacerbate operational issues related to fouling, slagging, and corrosion in biomass combustion facilities, as mentioned previously [3]. Profiling and quantifying the devolatilization behavior of potassium have become crucial procedures to mitigate the above issues in biomass combustion.

A research team at the University of Leeds measured and modeled the emissions of potassium during the combustion processes of biomass particles or pellets. Jones et al. [30] first measured potassium emissions by emission spectroscopy. The flame generated by burning biomass particles in a Méker burner was focused onto a monochromator, with the grating set to a wavelength of 766.5 nm, which is the characteristic wavelength of atomic potassium emission. A photo-multiplier tube recorded the detected wavelength's intensity. As shown in Figure 3, the results of the K emission measurements indicate three phases of potassium evolution. The first phase is the devolatilization of potassium. The second phase is the char combustion stage, while the third phase is the "ash-cooking" stage at the end of combustion. The last phase is the shrinking of the particle due to ash attrition.

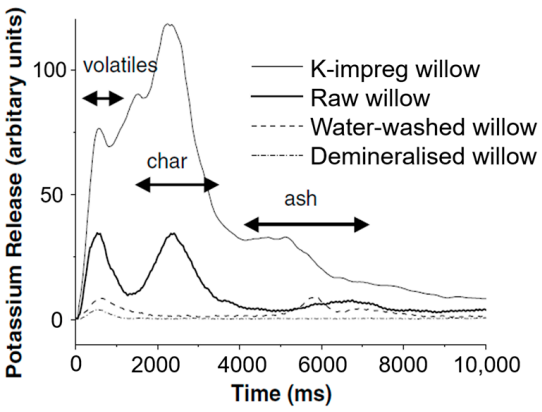

Figure 3. Examples of potassium emission profiles from willow with different pre-treatments. Reprinted with permission from Ref. [21]. 2005, Elsevier.

Similar results were observed in separate investigations for single biomass particle combustion of thirteen solid biomass fuels [31–33]. A band-pass interference filter (766 nm centered wavelength) and a low-cost photo-diode replaced the monochromator. An amplifier converted the output from the photo-diode to the radiative intensity. A second

photo-diode filter (750 nm centered wavelength) measured the background radiation intensity. The resulting spectrum is a subtraction of the 750 nm signal from the 766 nm signal, as shown in Figure 4. Similar to Figure 3, Figure 4 shows the three main stages of the combustion and potassium devolatilization profile: first, a low emission rate of potassium, followed by the char combustion stage with an increase and subsequent peak in the potassium emission rate; then, an exponential decay of the potassium emissions during the "ash-cooking" stage, which is dependent on the amount of ash content in the type of biomass. Using the same emission spectroscopy system, the effects of aluminosilicates on the gaseous concentrations of potassium from biomass pellets combustion were investigated in a separate lab burner [34]. The results indicated that the addition of aluminosilicate reduced the potassium emitted from the biomass pellets, especially during the char combustion and "ash-cooking" stages, as the potassium and aluminosilicates were bound in the ash.

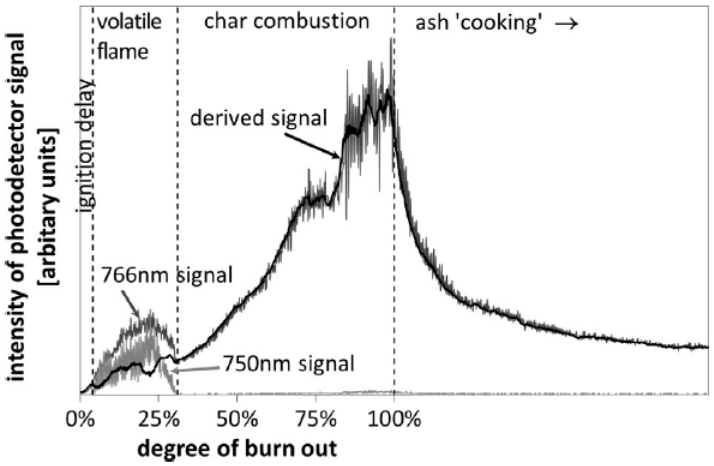

Figure 4. The three combustion phases of a willow particle after the subtraction of the background intensity. Adapted with permission from Ref. [32]. 2016, Elsevier.

The above studies summarized the setup and results from combustion processes using the SES passive measurement method, from which the evolution of the potassium emissions was characterized into three main phases: devolatilization, char combustion, and the ashing stage. However, the results are qualitative, and the application of such systems in an industrial setting for on-line, quantitative measurements to provide information for implementing slagging/fouling mitigation measures would not be possible. Calibration of such passive measurement methods before deployment is needed in order for the results to be meaningful.

The calibration can be performed by correlating the line emission intensities to known gaseous alkali metal concentrations. This was achieved with a flat flame burner by the authors from the Huazhong University of Science and Technology (HUST). Figure 5 shows the calibration experiment using a laminar flat flame, seeded with known concentrations of potassium chloride (KCl) solution. The line-of-sight spontaneous emission spectra of the flame were detected with spectrometers. The digital signals from the spectrometer were processed through software to obtain the spectral radiative intensity. An algorithm then correlated the intensity and temperature with the gaseous K concentration. Thus, with the alkali metals' spectral intensities calibrated to known concentrations, the gaseous concentrations of the alkali metals in other flames could be obtained [35,36].

Using the above calibration method, He et al. [35] measured the gaseous concentration of potassium, temperature, and thermal radiation from the combustion of camphorwood and rice husk pellets. Figure 6 shows the three typical stages of biomass pellet combustion as mentioned in Section 3.1, delineated by the inflection points of the curves for the gaseous potassium concentration, temperature, and thermal radiation. The results also show that

the volatile matter and silica oxide contents in the biomass pellets have significant effects on the devolatilization of potassium in the last two stages.

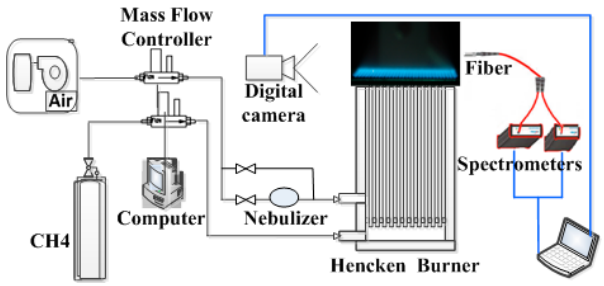

Figure 5. Experimental setup of calibration for determination of gaseous K concentration.

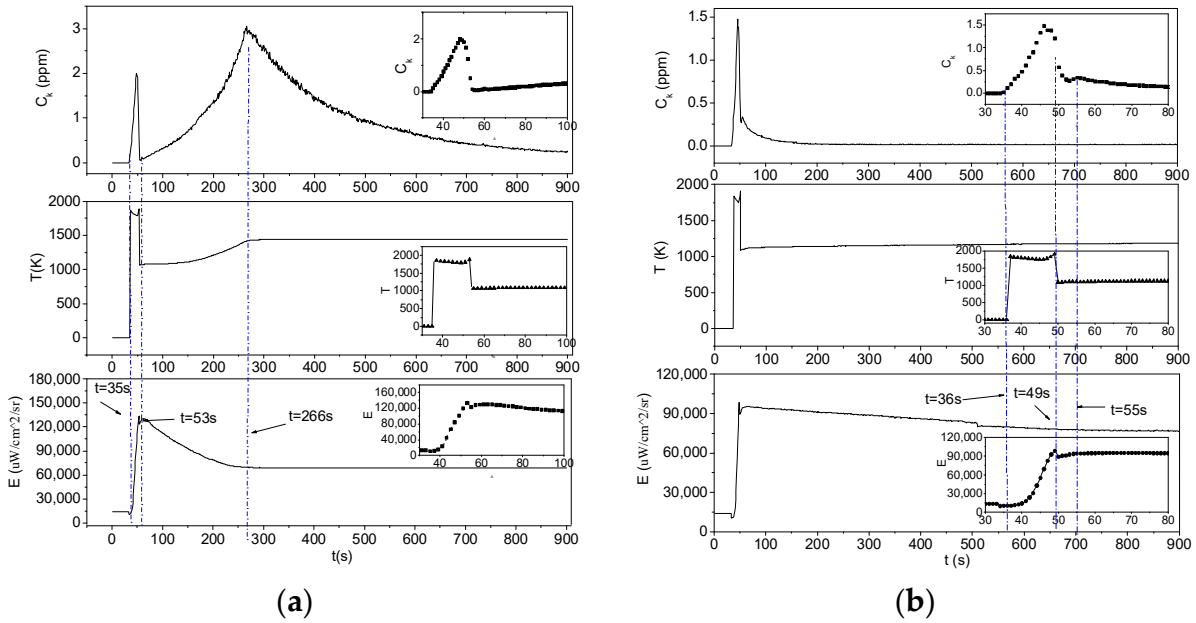

(**a**) (**b**)

Figure 6. Temporal profiles of gaseous potassium concentration, temperature, and thermal radiation of (**a**) camphorwood and (**b**) rice husk. Reprinted with permission from Ref. [35]. 2019, Elsevier.

Figure 6 shows the quantitative gaseous concentration of potassium, as opposed to Figures 3 and 4, which only show arbitrary intensity units. Additionally, other studies used the intensity of the alkali metals obtained by SES as a tentative indicator [37], which was correlated with ICP-MS analysis of the ash [38] for the prediction of potassium concentration in biomass fuels [39]. However, the applicability of the SES method for profiling the spatial and temporal alkali metal concentrations on a macroscale (in industrial settings) remains to be proven. Because large, industrial-scale biomass combustion facilities are not common, the following section presents examples of the deployment of the SES in coal and municipal solid waste combustion facilities.

3.2. Coal Combustion

Chinese Zhundong, Australian lignite coals, etc. [40,41], contain a higher amount of alkali metals, resulting in slagging and fouling in boilers and furnaces due to reasons discussed in the earlier sections. The devolatilization characteristics of gaseous sodium strongly depend on combustion temperature and coal composition. Therefore, as mentioned earlier, it is critical to quantitatively investigate the alkali metal emission behavior or devolatilization characteristics, along with the temperature variation in coal combustion as a first step to mitigate slagging and fouling.

Earlier studies measured the flame emissivities and temperature in industrial furnaces [26–28,42], in which the emission lines of alkali metals were not investigated in detail. In recent years, the ignition and combustion characteristics of Zhundong coal was investigated in lab-scale combustion facilities through the SES method. Zhang et al. [43] used an emission spectrometer to obtain the spontaneous emission spectrum from a single particle ignition in a horizontal tube furnace. Figure 7 shows the temporal profile for the 589 nm wavelength line emission for raw (ZDL-Raw), water-washed (ZDL-WW), and acid-washed (ZDL-AW) Zhundong coal samples. The significant increase in the intensity indicates the devolatilization of sodium during the ignition phase of the lignite. The line emission intensity at 589 nm decreases subsequently, indicating that the sodium concentration decreases with an increase in time. Sodium is soluble in water and more so in acidic solutions. Thus, the water- and acid-washed Zhundong coals showed significantly lower sodium emissions (Figure 7). In addition, Dong et al. [44] also analyzed the temporal emission profile by detecting the atomic emission spectrum of alkali metals, and found that the presence of different potassium compounds was the main factor that affected the emission rate. The results show that the SES method is sensitive to the changes to alkali metals in the fuels that have undergone pre-treatment methods.

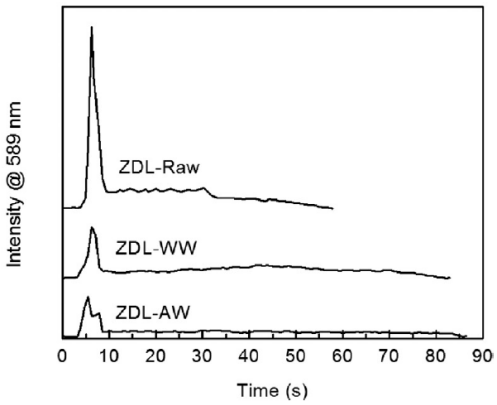

Figure 7. Temporal variations in flame emission intensity at 589 nm of burning ZDL-Raw, ZDL-WW, and ZDL-AW particles. Adapted with permission from Ref. [43]. 2017, Elsevier.

Based on the studies of measuring potassium emissions in biomass combustion by SES [35], the authors from HUST implemented the calibration procedure for quantifying the gaseous sodium concentration in the flame as well, and performed in situ monitoring of the gaseous sodium concentration for two types of Zhundong coal: ZD-WCW and ZD-HSQ [45–47]. These coals have different ash compositions, and were combusted in a lab-scale Hencken flat flame burner. Figure 8 shows the sodium emission profile during the three stages of evolution mentioned earlier (similar to that of potassium), with higher silica-to-aluminum (Si/Al) ratios in the ash (ZD-HSQ) suppressing the sodium emissions during the ash-cooking stage.

Using the calibration procedure to determine the gaseous alkali metal concentrations, a portable spontaneous emission spectroscopy (SES) system was constructed by the authors from HUST, and was deployed to two 1200 t/h boilers (FK1 and FK2) and two 480 t/h boilers coal-fired boilers (SD1 and SD2). The portable SES system consists of an optical emission spectrometer with optical fibers, a collimating lens, and a tablet personal computer. A dedicated application software was developed so that the tablet calculates and displays the gaseous sodium concentration and combustion temperature [45,47]. From the measurements, the sodium concentration profiles with respect to the width and height (labelled #1, #2, etc.) of the industrial boilers are obtained (Figure 9). The figure also shows that the higher silica and aluminum content in the GLT and ZN coals reduces the emissions of sodium in the burner zone of the boilers. When the temperature and furnace load increased, the portable SES also indicates that a higher amount of sodium was emitted.

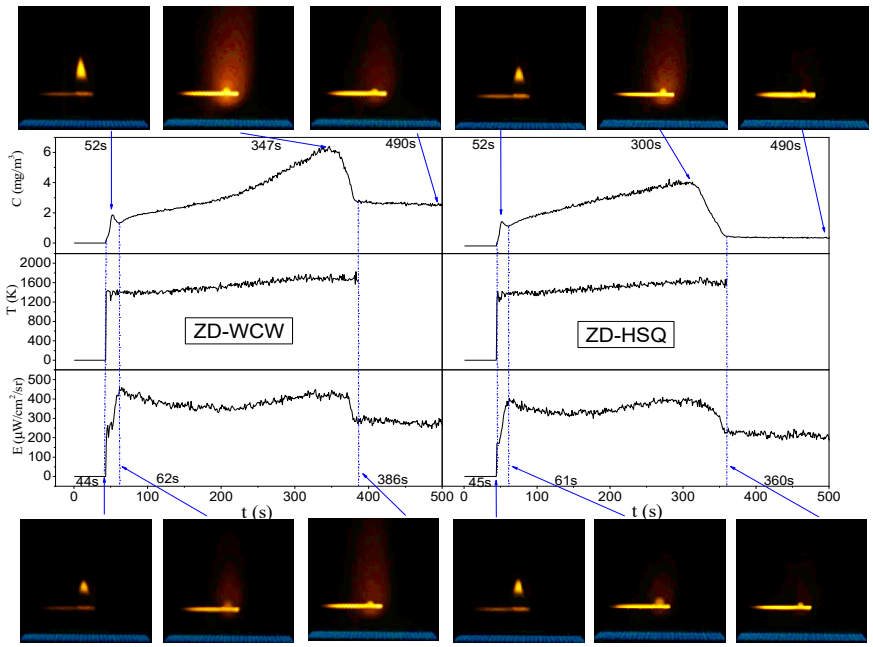

Figure 8. Measured Na concentration, temperature, and thermal radiation of Zhundong coal particles combustion. Adapted with permission from Ref. [45]. 2021, Elsevier.

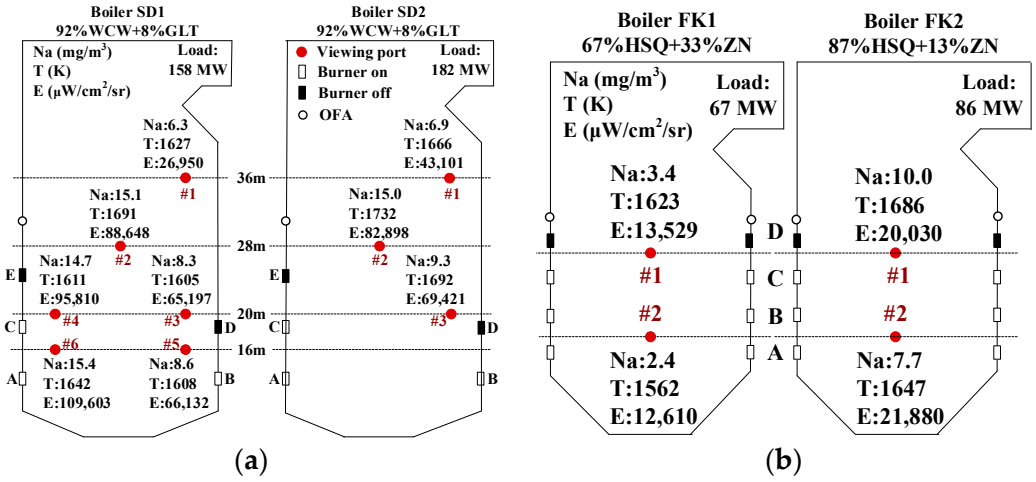

Figure 9. Measured Na concentration, temperature, and thermal radiation (**a**) in boilers SD1 and SD2; (**b**) in boilers FK1 and FK2. Reprinted with permission from Ref. [45]. 2021, Elsevier.

Figure 10 shows that the portable SES system is able to provide a macroscopic profile of the gaseous alkali metal concentration, as long as visual or optical access to the flame is available to provide line-of-sight measurements. A strong correlation between the alkali metal concentration and the combustion temperature was also observed.

In a second example of an industrial application of the SES system, the authors from HUST performed measurements in a 20 kW, slagging-type cyclone-fired combustor and a 300 MW slag-tapping boiler [47]. In the cyclone combustor, Zhundong FK and HSQ coals were used, and the effect of the temperature on the sodium's devolatilization was investigated by varying the temperature from 1100 to 1400 K. For the 300 MW boiler, the measurements quantified the effect of the coals' sodium content on its emission characteristics. The details of coal properties and experimental procedures are available in [47]. Figure 11a shows that for the 20 kW cyclone combustor, when the combustion temperatures for both FK and HSQ coals increase, the gaseous sodium emitted from the HSQ coal is much higher than that of FK coal, due to the sodium content in HSQ coal. Figure 11b

shows the temperature and sodium concentration from two viewing ports (#1 and #2) in the burn-out chamber of the 300 MW slag-tapping boiler. The combustion temperature remains relatively constant with the increase in salt content, but the gaseous-phase sodium concentration increases. This represents an insignificant correlation between the gaseous alkali metal concentration and the combustion temperature for a large industrial-scale boiler, possibly because the line-of-sight measurement point coincides with the lower emission rates of the combustion stage, i.e., during the initial ignition or ash-cooking stage (refer Figure 3 to Figure 4, and Figure 6 to Figure 7). Nevertheless, the next section presents an example where the gaseous alkali metal concentration on a macroscopic or industrial scale is obtained using the SES method, and a strong correlation with the operation parameters was observed.

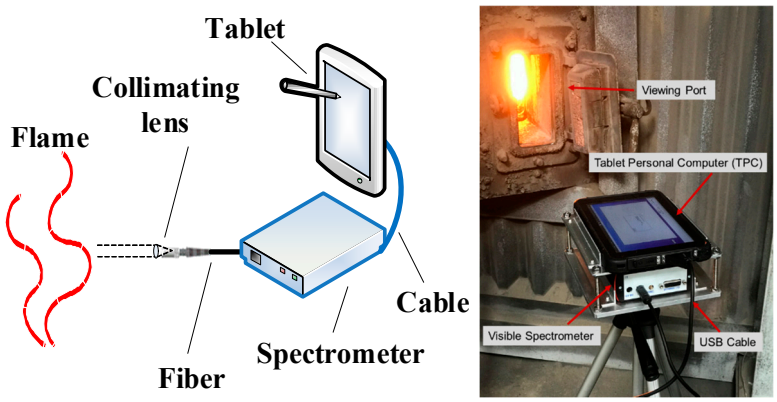

Figure 10. Schematic diagram and photo of the portable spectral analysis system.

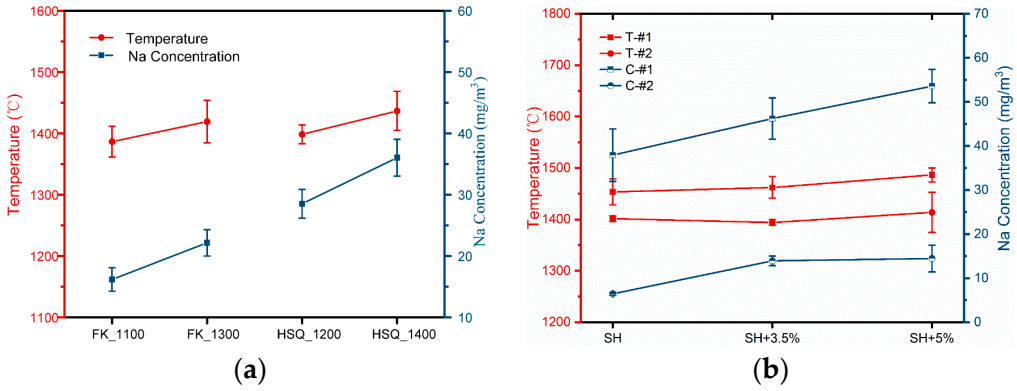

Figure 11. Measured Na concentration and temperature with standard deviations (**a**) in a 20 kW slag-tapping combustor and (**b**) in a slagging boiler of a 300 MW power generation unit. Adapted with permission from Ref. [47]. 2022, MDPI.

3.3. Municipal Solid Waste Combustion

Incineration is used for the disposal of municipal solid waste (MSW), but dioxin emissions, slagging, and corrosion are problematic issues related to operating a MSW incinerator. Similar to coal and biomass, MSW also contains a high content of alkali metals that cause slagging and fouling [48,49]. For reasons already mentioned above, the in situ monitoring of real-time gaseous alkali metal concentrations has become critical to mitigate such operational issues.

Authors from HUST measured the temperature and emissivity from two MSW incinerators using optical emission spectrometers [27,50], with results showing significant potassium and sodium emissions from the flames. There was also a strong correlation between temperatures and the line intensities of the alkali metals and the primary air flow rates. Based on this preliminary work, authors from the HUST group also deployed

the portable SES system for the determination of alkali metal concentrations from two mechanical grate waste incinerator plants in Wuhan and Xuzhou [51]. The experimental results showed that the composition of the waste affected the gaseous alkali metal concentrations, and was closely correlated with the temperature. This is shown in Figure 12, and was caused by the higher volatile matter content in Wuhan's MSW composition (61.47%) compared to Xuzhou's (30.83%), increasing the alkali metal emissions. This observation was validated with corresponding concentrations in the fly ash. Recently, a research group in Zhejiang University also investigated the emission characteristics of potassium and sodium during MSW pellet combustion using the SES technique [52], aiming to improve the understanding of the devolatilization characteristics of potassium and sodium during the combustion of various MSW fractions. Their results revealed the difference in the transformation processes of biomass-based materials and plastics (textiles) in the three stages of combustion.

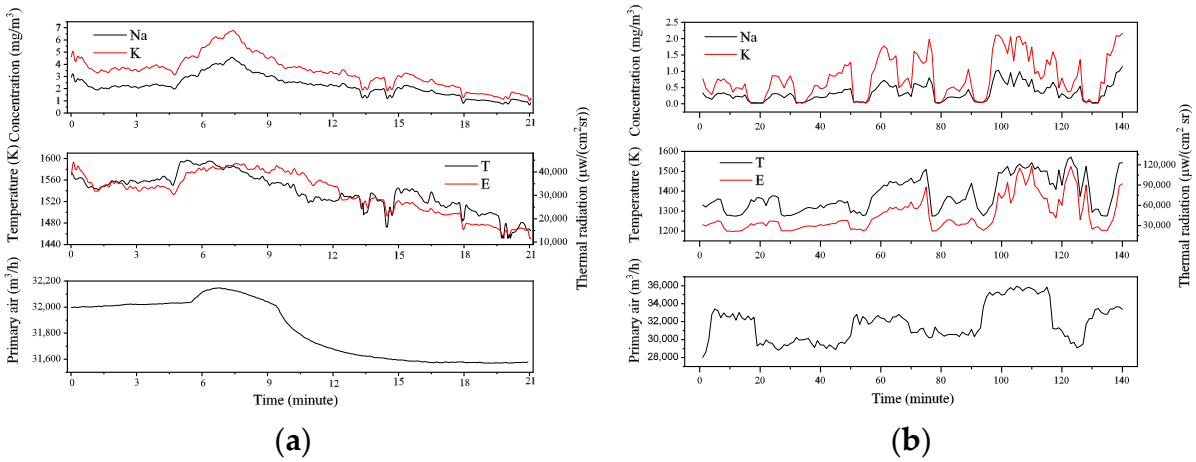

Figure 12. Measured K and Na concentration, temperature, thermal radiation, and primary air flow in MSW incinerators located (**a**) in Wuhan and (**b**) in Xuzhou. Reprinted with permission from Ref. [51]. 2020, Elsevier.

4. Challenges and Recommendations

This article reviews the procedures for the calibration and quantification of gaseous alkali metal concentrations for the SES passive measurement method. Deployment of the method to obtain macro- or industrial-scale spatial and temporal profiles of gaseous alkali metal concentrations is presented as well. However, several challenges for further propagation of the method still remain. For instance, if the gaseous sodium concentration profile such as that shown in Figure 10 is the main requirement of the client or the plant operators, it should be remembered that the sodium concentrations presented in Figure 10 were not measured simultaneously, and the concentration for point #1 may have changed by the time measurements for all points (up to #6) have been completed. The correlation of the alkali metal concentrations with the combustion parameters in real time may become arbitrary. Even if multiple SES systems were installed at all points for simultaneous measurement, and these were automated as well, it is not feasible for the plant to have all measurement points with optical or visual access to the flames open continuously at all times.

To reduce the manual labor required for performing the measurements as swiftly as possible (so as to reduce temporal variations), and to reduce the need for continuous optical access, machine learning techniques could be used to provide predictive analytics of alkali metal concentrations. This method would require preliminary datasets from historical measurements, serving as an input to train the machine learning model, providing a prediction of what the alkali metal concentrations might be within the constraints of the data input and the corresponding operating conditions. Such methods have been used to predict the characteristics of crude bio-oil from pyrolysis, with the reaction conditions

and chemical compositions as the input data for the machine learning model [53]. More information on the application of machine learning for other applications, particularly for yield optimization and process control for thermochemical conversion of biomass, is available from [54].

Whilst the passive measurement method provides quantitative information for mitigation measures to be implemented promptly, the issues caused by alkali metals are not avoidable. To avoid such operational issues would require analysis of the fuels, such that fuels with a high alkali metal content are not used. If the source and supply of a fuel are located in a remote location, the fuel needs to be collected and sent to an offsite lab for analysis, which can be a time-consuming process. This is especially the case for biomass, as the supply may be from different locations. Another method to reduce the time and costs for offsite analysis of the fuel would be to measure the alkali metal content on-site using a handheld, portable analyzer. This would mean that the fuel does not need to be sent to an offsite laboratory, nor do the plant owners or fuel procurement executives need to travel to a remote location to source or collect fuel samples, only for the samples to be sent for analysis at a separate laboratory. Current portable analyzers on the market are mainly meant for metallic materials and the mining industry [55,56]. For the detection of non-metallic materials such as solid coal or biomass, active measurement techniques using lasers as the excitation source need to be miniaturized and mobilized. External-cavity diode lasers (ECDLs) are one such device. ECDLs are small, relatively cheaper in cost, and the wavelength is tunable, but ECDLs are still under development, with their own issues that need to be addressed [57], and so far (to the authors knowledge), no ECDLs have been developed for the detection of alkali metals from solid biomass and coal, although diode lasers have been used for other purposes, such as the measurement of CO_2 at high temperatures [58].

5. Conclusions

This article has described the principles and calibration procedures for the quantitative measurement of gaseous alkali metal concentrations. This article has also reviewed the applications of passive spontaneous emission spectroscopy in industrial-scale settings to obtain macroscale spatial and temporal profiles of alkali metal concentrations. The review shows that several spontaneous emission spectroscopy systems, developed by the authors from the Huazhong University of Science and Technology (HUST), are inexpensive, portable, and useful for measuring the alkali metal content, providing near-real-time information for implementing slagging- and fouling-mitigation measures. This review also discusses the challenges of the further propagation of the system, recommending that machine learning techniques are incorporated to reduce temporal variations that may occur during the measurement process. Smaller, portable handheld devices may be another future development in order for the alkali metals in solid fuels to be quantified in remote locations, reducing the time-consuming process of their analysis.

Author Contributions: Formal analysis and data curation, W.L.; methodology and software, C.Y.; investigation, X.L.;writing—original draft preparation, Y.P.; writing—review and editing, M.L.; conceptualization and funding acquisition, C.L. All authors have read and agreed to the published version of the manuscript.

Funding: This research was funded by the National Key Research and Development Program (2022YFB4202002), National Natural Science Foundation of China (No. 51827808).

Conflicts of Interest: The authors declare no conflict of interest.

References

1. Bryers, R.W. Fireside slagging, fouling, and high-temperature corrosion of heat-transfer surface due to impurities in steam-raising fuels. *Prog. Energy Combust. Sci.* **1996**, *22*, 29–120. [CrossRef]
2. Li, X.; Li, J.; Wu, G.G.; Bai, Z.Q.; Li, W. Clean and efficient utilization of sodium-rich Zhundong coals in China: Behaviors of sodium species during thermal conversion processes. *Fuel* **2018**, *218*, 162–173. [CrossRef]

3. Niu, Y.Q.; Tan, H.Z.; Hui, S.E. Ash-related issues during biomass combustion: Alkali induced slagging, silicate melt-induced slagging (ash fusion), agglomeration, corrosion, ash utilization, and related countermeasures. *Prog. Energy Combust. Sci.* **2016**, *52*, 1–61. [CrossRef]
4. Reinmöller, M.; Li, K.X.; Laabs, M. Methods for the determination of composition, mineral phases, and process-relevant behavior of ashes and its modeling: A case study for an alkali-rich ash. *J. Energy Inst.* **2022**, *100*, 137–147. [CrossRef]
5. Abelha, P.; Vilela, C.M.; Nanou, P. Combustion improvements of upgraded biomass by washing and torrefaction. *Fuel* **2019**, *253*, 1018–1033. [CrossRef]
6. Ma, X.W.; Li, F.H.; Ma, M.J. Fusion characteristics of blended ash from Changzhi coal and biomass. *J. Fuel Chem. Technol.* **2018**, *46*, 129–137. [CrossRef]
7. Fatehi, H.; Weng, W.B.; Li, Z.S.; Bai, X.S.; Marcus, A. Recent development in numerical simulations and experimental studies of biomass thermochemical conversion. *Energy Fuels* **2021**, *35*, 6940–6963. [CrossRef]
8. Van Eyk, P.J.; Ashman, P.J.; Alwahabi, Z.T.; Nathan, G.J. Quantitative measurement of atomic sodium in the plume of a single burning coal particle. *Combust. Flame* **2008**, *155*, 529–537. [CrossRef]
9. Hsu, L.J.; Alwahabi, Z.T.; Nathan, G.J.; Li, Y.; Li, Z.S.; Aldén, M. Sodium and potassium released from burning particles of brown coal and pine wood in a laminar premixed methane flame using quantitative Laser-Induced Breakdown Spectroscopy. *Appl. Spectrosc.* **2011**, *65*, 684–691. [CrossRef]
10. Forsberg, C.; Brostrom, M.; Backman, R.; Edvardsson, E.; Badiei, S.; Berg, M.; Kassman, H. Principle, calibration and application of the in-situ alkali chloride monitor (IACM). *Rev. Sci. Instrum.* **2009**, *80*, 023104. [CrossRef]
11. Sepman, A.; Ögren, Y.; Qu, Z.; Wiinikka, H.; Schmidt, F.M. Real-time in situ multi-parameter TDLAS sensing in the reactor core of an entrained-flow biomass gasifier. *Proc. Combust. Inst.* **2017**, *36*, 4541–4548. [CrossRef]
12. Erbel, C.; Mayerhofer, M.; Monkhouse, P.; Gaderer, M. Continuous in situ measurements of alkali species in the gasification of biomass. *Proc. Combust. Inst.* **2013**, *34*, 2331–2338.
13. García-Armingol, T.; Ballester, J. Influence of fuel composition on chemiluminescence emission in premixed flames of $CH_4/CO_2/H_2/CO$ blends. *Int. J. Hydrog. Energy* **2014**, *39*, 20255–20265. [CrossRef]
14. Lim, M.; Matsuoka., L. Quantitative analysis and speciation of alkali metal emissions from biomass combustion in a 150 kWth furnace by optical emission spectroscopy. *Chem. Eng. Commun.* **2021**, *208*, 453–462. [CrossRef]
15. Ballester, J.; García-Armingol, T. Diagnostic techniques for the monitoring and control of practical flames. *Prog. Energy Comb. Sci.* **2010**, *36*, 375–411. [CrossRef]
16. Lou, C.; Zang, L.D.; Pu, Y.; Zhang, Z.N.; Li, Z.C.; Chen, P.F. Research advances in passive techniques for combustion diagnostics based on analysis of spontaneous emission radiation. *J. Exp. Fluid Mech.* **2021**, *35*, 1–17.
17. Gaydon, A.G. *The Spectroscopy of Flames*, 2nd ed.; Chapman and Hall: London, UK, 1974.
18. Whiting, E.E. An empirical approximation to the Voigt profile. *J. Quant. Spectrosc. Radiat. Transfer* **1968**, *8*, 1379–1384.
19. Di. Marco, V.B.; Bombi, G.G. Mathematical functions for the representation of chromatographic peaks. *J. Chromatogr. A* **2001**, *931*, 1–30. [CrossRef]
20. AlOmar., A.A.S. Line width at half maximum of the Voigt profile in terms of Gaussian and Lorentzian widths: Normalization, asymptotic expansion, and chebyshev approximation. *Optik* **2020**, *203*, 163919. [CrossRef]
21. Kohse-Höinghaus, K.; Barlow, R.S.; Aldén, M. Combustion at the focus: Laser diagnostics and control. *Proc. Combust. Inst.* **2005**, *30*, 89–123. [CrossRef]
22. Monkhouse, P. On-line spectroscopic and spectrometric methods for the determination of metal species in industrial processes. *Prog. Energy Combust. Sci.* **2011**, *37*, 125–171. [CrossRef]
23. Worsfold, P.; Townshend, A.; Poole, C.F. *Encyclopedia of Analytical Science*, 3rd ed.; Elsevier: Amsterdam, The Netherlands, 2019.
24. Arias, L.; Torres, S.; Ngendakumana, D.S.P. On the spectral bands measurements for combustion monitoring. *Combust. Flame* **2011**, *158*, 423–433. [CrossRef]
25. Keyvan, S.; Rossow, R.; Romero, C. Blackbody-based calibration for temperature calculations in the visible and near-IR spectral ranges using a spectrometer. *Fuel.* **2006**, *85*, 796–802. [CrossRef]
26. Sun, Y.P.; Lou, C.; Zhou, H.C. A simple judgment method of gray property of flames based on spectral analysis and the two-color method for measurements of temperatures and emissivity. *Proc. Combust. Institute.* **2011**, *33*, 735–741. [CrossRef]
27. Yan, W.J.; Zhou, H.C.; Jiang, Z.W.; Lou, C.; Zhang, X.K.; Chen, D.L. Experiments on measurement of temperature and emissivity of municipal solid waste (MSW) combustion by spectral analysis and image processing in visible spectrum. *Energy Fuel.* **2013**, *27*, 6754–6762. [CrossRef]
28. Parameswaran, T.; Hughes, R.; Gogolek, P.; Hughes, P. Gasification temperature measurement with flame emission spectroscopy. *Fuel* **2014**, *134*, 579–587. [CrossRef]
29. Ebdon, L.; Evans, E.H.; Fisher, A.; Hill, S.J. *An Introduction to Analytical Atomic Spectrometry*; Wiley: New York, NY, USA, 1998.
30. Jones, J.M.; Darvell, L.I.; Bridgeman, T.G.; Pourkashanian, M.; Williams, A. An investigation of the thermal and catalytic behaviour of potassium in biomass combustion. *Proc. Combust. Inst.* **2007**, *31*, 1955–1963. [CrossRef]
31. Mason, P.E.; Darvell, L.I.; Jones, J.M.; Pourkashanian, M.; Williams, A. Single particle flame-combustion studies on solid biomass fuels. *Fuel* **2015**, *151*, 21–30. [CrossRef]
32. Mason, P.E.; Darvell, L.I.; Jones, J.M.; Williams, A. Observations on the release of gas-phase potassium during the combustion of single particles of biomass. *Fuel* **2016**, *182*, 110–117. [CrossRef]

33. Mason, P.E.; Jones, J.M.; Darvell, L.I.; Williams, A. Gas phase potassium release from a single particle of biomass during high temperature combustion. *Proc. Combust. Inst.* **2017**, *36*, 2207–2215. [CrossRef]
34. Clery, D.S.; Mason, P.E.; Rayner, C.M.; Jones, J.M. The effects of an additive on the release of potassium in biomass combustion. *Fuel* **2018**, *214*, 647–655. [CrossRef]
35. He, Z.L.; Lou, C.; Fu, J.T.; Lim, M. Experimental investigation on temporal release of potassium from biomass pellet combustion by flame emission spectroscopy. *Fuel* **2019**, *253*, 1378–1384. [CrossRef]
36. Li, K.Y.; Yan, W.J.; Huang, X.L.; Yu, L.B.; Chen, Y.M.; Lou, C. In-situ measurement of temperature and potassium concentration during the combustion of biomass pellets based on the emission spectrum. *Fuel* **2021**, *289*, 119863. [CrossRef]
37. Lim, M.; Ahmad, Z.S.Z.; Hamdan, H. Biomass combustion: Potassium and sodium flame emission spectra and composition in ash. *J. Jpn. Inst. Energy* **2017**, *96*, 367–371. [CrossRef]
38. Paulauskas, R.; Striūgas, N.; Sadeckas, M.; Sommersacher, P.; Retschitzegger, S.; Kienzl, N. Online determination of potassium and sodium release behaviour during single particle biomass combustion by FES and ICP-MS. *Sci. Total Environ.* **2020**, *746*, 141162. [CrossRef]
39. Li, X.L.; Han, C.X.; Lu, G.; Yan, Y. Online dynamic prediction of potassium concentration in biomass fuels through flame spectroscopic analysis and recurrent neural network modelling. *Fuel* **2021**, *304*, 121376. [CrossRef]
40. Long, X.F.; Li, J.B.; Wang, H.J. The morphological and mineralogical characteristics and thermal conductivity of ash deposits in a 220 MW CFBB firing Zhundong lignite. *Energy* **2023**, *263*, 125842. [CrossRef]
41. Guo, S.; Jiang, Y.F.; Yu, Z.L.; Zhao, J.T. Correlating the sodium release with coal compositions during combustion of sodium-rich coals. *Fuel* **2017**, *196*, 252–260. [CrossRef]
42. Cai, X.S.; Cheng, Z.H.; Wang, S.M. Flame measurement and combustion diagnoses with spectrum analysis. In *AIP Conference Proceedings*; American Institute of Physics: Melville, NY, USA, 2007.
43. Zhang, Z.Z.; Zhu, M.M.; Zhang, Y.; Setyawan, H.Y.; Li, J.B.; Zhang, D.K. Ignition and combustion characteristics of single particles of Zhundong lignite: Effect of water and acid washing. *Proc. Combust. Inst.* **2017**, *36*, 2139–2146.
44. Dong, M.R.; Luo, F.S.; Huang, M.; Li, S.S.; Zhao, W.H.; Lu, J.D. Study on the ignition characteristics and alkali release of single coal particles with additional different forms of potassium. *Fuel Process. Technol.* **2020**, *203*, 106385. [CrossRef]
45. Lou, C.; Pu, Y.; Zhao, Y.G.; Bai, Y.; Yao, B.; Yu, D.X. An in-situ method for time-resolved sodium release behaviour during coal combustion and its application in industrial coal-fired boilers. *Proc. Combust. Institute.* **2021**, *38*, 4199–4206. [CrossRef]
46. Li, K.Y.; Yan, W.J.; Yu, L.B.; Huang, X.L.; Chen, Y.M.; Zhou, H.C.; Zheng, S.; Lou, C. Simultaneous determination of Na concentration and temperature during Zhundong coal combustion using the radiation spectrum. *Energy Fuels* **2021**, *35*, 3348–3359. [CrossRef]
47. Jing, X.H.; Pu, Y.; Li, Z.; Tang, Q.; Yao, B.; Fu, P.; Lou, C.; Lim, M. Experimental investigation of gaseous sodium release in slag-tapping coal-fired furnaces by spontaneous emission spectroscopy. *Energies* **2022**, *15*, 4165. [CrossRef]
48. Zhao, J.; Li, B.; Wei, X.L.; Zhang, Y.F. Slagging characteristics caused by alkali and alkaline earth metals during municipal solid waste and sewage sludge co-incineration]. *Energy* **2020**, *202*, 117773. [CrossRef]
49. Zhao, Y.; Liu, G.C.; Huang, J.J. Sorbents for high-temperature removal of alkali metals and HCl from municipal solid waste derived syngas. *Fuel* **2022**, *321*, 124058. [CrossRef]
50. Yan, W.J.; Lou, C.; Cheng, Q.; Zhao, P.T.; Zhang, X.Y. In Situ Measurement of alkali metals in an MSW incinerator using a spontaneous emission spectrum. *Appl. Sci.* **2017**, *7*, 263. [CrossRef]
51. He, X.H.; Lou, C.; Qiao, Y.; Lim, M. In-situ measurement of temperature and alkali metal concentration in municipal solid waste incinerators using flame emission spectroscopy. *Waste Manag.* **2020**, *102*, 486–491. [CrossRef]
52. He, J.J.; Li, J.Y.; Huang, Q.X.; Yan, J.H. Release characteristics of potassium and sodium during pellet combustion of typical MSW fractions using the FES method. *Combust. Flame* **2022**, *244*, 112233. [CrossRef]
53. Zhang, T.H.; Cao, D.Y.; Feng, X. Machine learning prediction of bio-oil characteristics quantitatively relating to biomass compositions and pyrolysis conditions. *Fuel* **2022**, *312*, 122812. [CrossRef]
54. Khan, M.; Raza, N.S.; Ullah, Z. Applications of machine learning in thermochemical conversion of biomass-A review. *Fuel* **2023**, *332*, 126055. [CrossRef]
55. Connors, B.; Somers, A.; Day, D. Application of handheld laser-induced breakdown spectroscopy (LIBS) to geochemical analysis. *Appl. Spectrosc.* **2016**, *70*, 810–815. [CrossRef]
56. Lemiere, B. A review of pXRF (field portable X-ray fluorescence) applications for applied geochemistry. *J. Geochem. Explor.* **2018**, *188*, 350–363. [CrossRef]
57. Han, J.J.; Zhang, J.; Shan, X.N.; Zhang, Y.W. High-power Narrow-linewidth 780 nm Diode Laser Based on External Cavity Feedback Technology of Volume Bragg Grating. *Optik* **2022**, *264*, 169455. [CrossRef]
58. Chen, J.Y.; Li, C.R.; Zhou, M. Measurement of CO_2 concentration at high-temperature based on tunable diode laser absorption spectroscopy. *Infrared Phys. Technol.* **2017**, *80*, 131–137. [CrossRef]